**Keywords:** chirality · gallium · self-assembly · supramolecular chemistry


[1] R. Krämer, J.-M. Lehn, A. De Cian, J. Fischer, *Angew. Chem.* **1993**, *105*, 764 – 768; *Angew. Chem. Int. Ed. Engl.* **1993**, *32*, 703 – 706.

[2] B. Hasenknopf, J.-M. Lehn, B. O. Kneisel, G. Baum, D. Fenske, *Angew. Chem.* **1996**, *108*, 1987 – 1990; *Angew. Chem. Int. Ed. Engl.* **1996**, *35*, 1838 – 1840.

[3] P. N. W. Baxter, J.-M. Lehn, K. Rissanen, *Chem. Commun.* **1997**, 1323 – 1324.

[4] F. M. Romero, R. Ziessel, A. Dupont-Gervais, A. Van Dorsselaer, *Chem. Commun.* **1996**, 551 – 553.

[5] C. Provent, S. Hewage, G. Brand, G. Bernardinelli, L. J. Charbonnière, A. F. Williams, *Angew. Chem.* **1997**, *109*, 1346 – 1348; *Angew. Chem. Int. Ed. Engl.* **1997**, *36*, 1287 – 1289.

[6] R. C. Scarrow, D. L. White, K. N. Raymond, *J. Am. Chem. Soc.* **1985**, *107*, 6540 – 6546.

[7] A. F. Williams, C. Piguet, G. Bernardinelli, *Angew. Chem.* **1991**, *103*, 1530 – 1533; *Angew. Chem. Int. Ed. Engl.* **1991**, *30*, 1490 – 1492.

[8] D. Zurita, P. Baret, J.-L. Pierre, *New J. Chem.* **1994**, *18*, 1143 – 1146.

[9] E. J. Enemark, T. D. P. Stack, *Angew. Chem.* **1995**, *107*, 1082 – 1084; *Angew. Chem. Int. Ed. Engl.* **1995**, *34*, 996 – 998.

[10] M. Albrecht, S. Kotila, *Angew. Chem.* **1995**, *107*, 2285 – 2287; *Angew. Chem. Int. Ed. Engl.* **1995**, *34*, 2134 – 2137.

[11] E. J. Enemark, T. D. P. Stack, *Inorg. Chem.* **1996**, *35*, 2719 – 2720.

[12] B. Kersting, M. Meyer, R. E. Powers, K. N. Raymond, *J. Am. Chem. Soc.* **1996**, *118*, 7221 – 7222.

[13] M. Albrecht, *Synlett* **1996**, 565 – 567.

[14] M. Albrecht, H. Röttele, P. Burger, *Chem. Eur. J.* **1996**, *2*, 1264 – 1268.

[15] M. Albrecht, S. Kotila, *Angew. Chem.* **1996**, *108*, 1299 – 1300; *Angew. Chem. Int. Ed. Engl.* **1996**, *35*, 1208 – 1210.

[16] V. A. Grillo, E. J. Seddon, C. M. Grant, G. Aromí, J. C. Bollinger, K. Folting, G. Christou, *Chem. Commun.* **1997**, 1561 – 1562.

[17] A. Williams, *Chem. Eur. J.* **1997**, *3*, 15 – 19.

[18] R. W. Saalfrank, A. Stark, K. Peters, H. G. von Schnering, *Angew. Chem.* **1988**, *100*, 878 – 880; *Angew. Chem. Int. Ed. Engl.* **1988**, *27*, 851 – 853.

[19] R. W. Saalfrank, A. Stark, M. Bremer, H.-U. Hummel, *Angew. Chem.* **1990**, *102*, 292 – 294; *Angew. Chem. Int. Ed. Engl.* **1990**, *29*, 311 – 314.

[20] R. W. Saalfrank, B. Hörner, D. Stalke, J. Salbeck, *Angew. Chem.* **1993**, *105*, 1223 – 1225; *Angew. Chem. Int. Ed. Engl.* **1993**, *32*, 1179 – 1182.

[21] R. W. Saalfrank, R. Burak, A. Breit, D. Stalke, R. Herbst-Irmer, J. Daub, M. Porsch, E. Bill, M. Müther, A. X. Trautwein, *Angew. Chem.* **1994**, *106*, 1697 – 1699; *Angew. Chem. Int. Ed. Engl.* **1994**, *33*, 1621 – 1623.

[22] T. Beissel, R. E. Powers, K. N. Raymond, *Angew. Chem.* **1996**, *108*, 1166 – 1168; *Angew. Chem. Int. Ed. Engl.* **1996**, *35*, 1084 – 1086.

[23] P. L. Jones, K. J. Byrom, J. C. Jeffery, J. A. McCleverty, M. D. Ward, *Chem. Commun.* **1997**, 1361 – 1362. A reviewer has pointed out that the reported 8:12 complex is a two-dimensional ring and that a three-dimensional 8:12 "molecular cube" is also possible.

[24] The crystal structure presented[11] is the structure of $(Et_4N)_6[Fe_2(L_{et}^{H,H})_3]\cdot 10H_2O$. The gallium structure is isomorphic. Crystal data for $(Et_4N)_6[Ga_2(L_{et}^{H,H})_3]\cdot 10H_2O$: $P3_221$ (no. 154) or $P3_121$ (no. 152), $a = 16.441(4)$, $c = 35.512(7)$ Å, $V = 8400(4)$ Å$^3$, $Z = 3$, $R(R_w) = 0.073(0.069)$.

[25] Since our initial report of this complex,[9] a crystal structure has been determined. Crystal data for $(TMI)_3[Ga_2(L_{pr}^{H,H})_3]\cdot 14H_2O$: $R\bar{3}c$ (no. 167), $a = 20.047(6)$, $c = 36.527(3)$ Å, $V = 12721(5)$ Å$^3$, $Z = 6$, $R(R_w) = 0.061(0.056)$. TMI = tetramethyldihydroimidazolinium.

[26] F. H. Dickey, W. Fickett, H. J. Lucas, *J. Am. Chem. Soc.* **1952**, *74*, 944 – 951.

[27] R. D. Gillard, *Tetrahedron* **1965**, *21*, 503 – 506.

[28] A single set of resonances is also consistent with a fluxional species or with a less symmetric species that has coinciding resonances. Fluxional behavior is highly unlikely given the lengthy equilibration time required to generate the complex and also the lack of fluxional behavior in $[Ga_2(L_{et}^{H,H})_3]^{6-}$ and $[Ga_2(L_{pr}^{H,H})_3]^{6-}$. This is demonstrated by diastereotopic signals in the $^1$H NMR spectra of these complexes. Diastereotopic protons are not observed in $[Ga_4(^{SS}L_{et}^{Me,Me})_6]^{12-}$ or in $[Ga_2(^{RR}L_{pr}^{Me,Me})_3]^{6-}$, but none are anticipated for these complexes. A less symmetric species is also unlikely as it would be expected that the various methyl and methylene protons of the ligand backbone would have very different chemical environments.

[29] J. Libman, Y. Tor, A. Shanzer, *J. Am. Chem. Soc.* **1987**, *109*, 5880 – 5881.

[30] W. Zarges, J. Hall, J.-M. Lehn, C. Bolm, *Helv. Chim. Acta* **1991**, *74*, 1843 – 1852.

[31] R. W. Saalfrank, M. Decker, F. Hampel, K. Peters, H. G. von Schnering, *Chem. Ber.* **1997**, *130*, 1309 – 1313.

[32] Several combinations of the two ligand enantiomers are possible: $[Ga_4(^{SS}L_{et}^{Me,Me})_a(^{RR}L_{et}^{Me,Me})_{6-a}]^{12-}$ $(0 \le a \le 6)$. If more than one of each enantiomer is present in a metal complex $(2 \le a \le 4)$, these ligands can be arranged in multiple orientations relative to each other. A list of all possible isomers is given in the supporting information on the WWW.

[33] Other examples of self-selectivity in self-assembly: R. Krämer, J.-M. Lehn, A. Marquis-Rigault, *Proc. Natl. Acad. Sci. USA* **1993**, *90*, 5394 – 5398; D. L. Caulder, K. N. Raymond, *Angew. Chem.* **1997**, *109*, 1508 – 1510; *Angew. Chem. Int. Ed. Engl.* **1997**, *36*, 1439 – 1442; M. A. Masood, E. J. Enemark, T. D. P. Stack, *ibid.* **1998**, *110*, 973 – 977 and **1998**, *37*, 928 – 932.

[34] AM1 calculations were performed with an idealized isopropylformamide unit.

[35] The additional carbon atom in the bridge of $^{RR}L_{pr}^{Me,Me}$ versus $^{SS}L_{et}^{Me,Me}$ provides one additional degree of rotational freedom in the ligand backbone. This degree of freedom allows an external projection of methyl groups while maintaining a favorable torsional conformation for C-N-C$^1$-Me. This degree of freedom is also likely to play an important role in the lack of selectivity in racemic $L_{pr}^{Me,Me}$.

[36] T. B. Karpishin, T. D. P. Stack, K. N. Raymond, *J. Am. Chem. Soc.* **1993**, *115*, 6115 – 6125.


# $B_4$ Tetrahedra for Aluminum Atoms—A Surprising Substitution in $\tau$-Borides $Ni_{20}Al_3B_6$ and $Ni_{20}AlB_{14}$**

Harald Hillebrecht* and Martin Ade

The solid-state chemistry of boron is remarakably diverse, which is attributed to the tendency of boron to form homonuclear interactions and numerous clusters.[1] Isolated boron atoms are usually observed for metal-rich borides with a ratio M:B > 2. Among this class of compounds, "$\tau$-borides" of the cubic $Cr_{23}C_6$-type (*Fm*3*m*, *cF*112[2]) represent the largest group with about 80 examples.[3] Usually ternary


[*] Prof. Dr. H. Hillebrecht,[+] Dr. M. Ade
Institut für Anorganische und Analytische Chemie
Albertstrasse 21, D-79104 Freiburg (Germany)

[+] New address:
Institut für Anorganische Chemie
Gerhard-Domagk-Strasse 1, 53121 Bonn (Germany)
Fax: (+49) 228 735-660
E-mail: hille@snchemie2.chemie.uni-bonn.de


[**] This work was supported by the Deutsche Forschungsgemeinschaft (DFG). We thank Prof Dr. G. Thiele (Freiburg) for his generous support of our work.

compounds of compositions $M_{20}M'_3B_6$ or $M_{21}M'_2B_6$ are observed, in which the major component M is frequently Ni or Co, and in some cases Cr, Mn, Fe, Ru, Re, or Ir. The minor component M′ can be either a main group metal (Li, Mg, Al, Ga, In, Ge, Sn, Sb), a rare earth metal (Er, Lu, Tm), or a transition metal. Several carbides, silicides,[4] germanides,[4] phosphides,[5] and binary borides ($Fe_{23}B_6$,[6] $Co_{23}B_6$[7]) can also be assigned this structure type. The $\tau$-borides are characterized predominantly by X-ray crystallography with powder methods. Only in the cases of $Ni_{20}Li_3B_6$ and $Co_{21}Ta_2B_6$ are structures based on single-crystal data.

Among these $\tau$-phases the Ni/Al/B system is a special case. Firstly, the lattice constants vary between 10.484 Å and 10.552 Å (800°C) and between 10.48 Å and 10.62 Å (1000°C) depending on the temperature of the synthesis. Secondly these variations of the lattice constants are connected to a remarkably large field of nonstoichiometry with respect to the boron content (10.48 Å: $Ni_{20}Al_3B_6$; 10.62 Å: $Ni_{20}Al_3B_{12}$). Stadelmaier et al. proposed that the enlargement of the unit cell with higher boron content might be attributed to the substitution of isolated boron atoms with a square-antiprismatical coordination by $B_2$ pairs. This would be very unusual for the structural chemistry of transition metal borides. In order to clarify the structure–chemical reasons for the variation of the boron content structure analyses based on single-crystal data were carried out across the whole range of existence of the $\tau$ phase.[12] Table 1 shows some of the results. Compositions were deduced from the refinement of site occupation factors and are in accordance with the corresponding conditions of formation (see Experimental Section).

Table 1. Results of structure analyses of $\tau$-borides in the system Ni/Al/B: $Ni_{20+x}Al_{3-x-2y}B_{6+8y}$ (compositions from refinement of occupation factors).

| Composition | Lattice constant | $x$ | $y$ |
|---|---|---|---|
| $Ni_{20.51(2)}Al_{2.49(2)}B_6$ | 10.4859(2) | 0.51(2) | 0[a] |
| $Ni_{20}Al_3B_6$ | 10.5110(4) | 0[a] | 0[a] |
| $Ni_{20}Al_{2.73(2)}B_{7.08(8)}$ | 10.5193(6) | 0[a] | 0.13(2) |
| $Ni_{20}Al_{2.40(4)}B_{8.4(2)}$ | 10.5689(2) | 0[a] | 0.30(2)) |
| $Ni_{20}Al_{1.12(3)}B_{13.5(1)}$ | 10.5895(3) | 0[a] | 0.94(2) |
| $Ni_{20}Al_{1.19(3)}B_{13.2(1)}$ | 10.5922(6) | 0[a] | 0.91(2) |
| $Ni_{20}AlB_{14}$ | 10.6167(3) | 0[a] | 1[a] |

[a] Value fixed.

With respect to the $Cr_{23}C_6$-type, $Ni_{20}Al_3B_6$ represents a ternary ordering variant (Figure 1). The two Ni sites form a NaCl-like pattern of $Ni_8$ cubes (site 32 f) and $Ni_{12}$ cuboctahedra (48 h). The Al positions are inside the cuboctahedra (4a) and inside the fourfold capped truncated tetrahedra ("Friauf"-polyhedra, Figure 2 a), which are formed by four triangular faces of the cuboctahedra and four corners of the cubes (site 8c). The boron atoms reside in a square antiprism built up by the square planes of one cuboctahedron and one cube. Starting from $Ni_{20}Al_3B_6$ the variation of the compositon can be explained by two different ways of substituting the Al atoms.

With increasing Ni content, some of the Al atoms on site 4a are replaced by Ni atoms: $Ni_{20+x}Al_{3-x}B_6$. This kind of

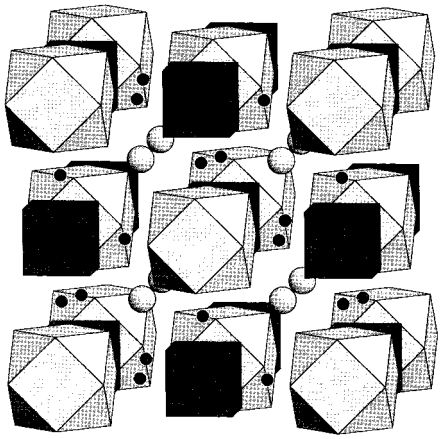

Figure 1. Crystal structure of the $\tau$-boride $Ni_{20}Al_3B_6$ with $Ni_{12}$ cuboctahedra (Ni2, 48h), $Ni_8$ cubes (Ni1, 32f), Al1 in the center of the cuboctahedra (4a), Al2: light spheres (8c), B: dark spheres (24e).

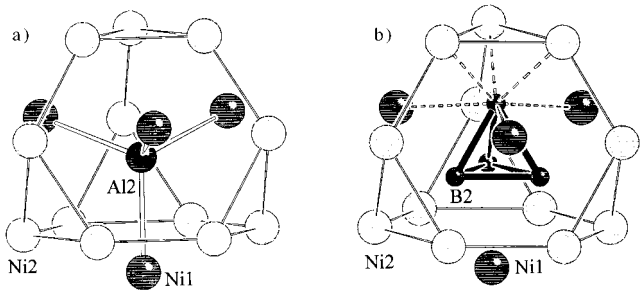


Figure 2. Coordination about a) Al2 in $Ni_{20}Al_3B_6$ [Al–Ni: $4 \times 2.411(1)$ Å, $12 \times 2.887(1)$ Å], and about b) $B_4$ tetrahedron in $Ni_{20}AlB_{14}$ [B–B: $3 \times 1.681(15)$ Å, B–Ni: $3 \times 2.093(8)$ Å, $3 \times 2.269(6)$ Å].

substitution is well known for $\tau$-borides and $\tau$-carbides.[3] Since Ni (1.246 Å) has a smaller atomic radius than Al (1.32 Å), this leads to a smaller lattice constant. For the single crystal with the highest Ni content (51(2)%) we found a lattice constant of 10.4859(2) Å. The complete replacement would result in the composition $Ni_{21}Al_2B_6$, but the minimum value of the lattice constant discounts the possibility of full substitution.

The variation of the boron content is achieved by a mechanism of substitution that is unique in solid-state chemistry. In the course of the structure analyses based on single-crystal data it became clear that the Al atoms on site 8c that are coordinated in a $4+12$-way are replaced by $B_4$ tetrahedra (Figure 2 b). This substitution takes place in a continuous way; that is, the electron density on site 8c decreases as the lattice constant and boron content increase. At the same time an additional maximum of electron density arises on a site 32 f with $x \approx 0.194$. If boron is located on this 32 f position, the resulting occupation factor and the deficit of aluminum at the 8c site are in a ratio of nearly 4:1. At the highest value of the lattice constant (10.6167(3) Å) the electron density on the 8c position is completely vanished. By placing boron on the 32 f site the refinement leads to full occupation. Therefore the composition $Ni_{20}AlB_{14}$ results as the end member of the series $Ni_{20}Al_{3-2y}B_{6+8y}$ with $y = 1$. The two ways of replacement are shown in Table 2. The changes of lattice constants caused by the substitution of Al by Ni and $B_4$

  1433-7851/98/3707-0936 $ 17.50+.50/0 

tetrahedra can be derived from the volume increments for the elements proposed by W. Biltz. [14] These patterns of substitutions are also supported by the experimental results, because by-products containing boron are observed if the ratio Ni:B is lower than 20:14.

Table 2. Representation of the two different ways of substitution in $Ni_{20+x}Al_{3-x-2y}B_{6+8y}$.

| Composition | 48h | 32f | 4a | 8c | 24e |
|---|---|---|---|---|---|
| $Ni_{21}Al_2B_6$ | $Ni_{12}$ | $Ni_8$ | **Ni** ↑ **x** | $Al_2$ | $B_6$ |
| $Ni_{20}Al_3B_6$ | $Ni_{12}$ | $Ni_8$ | **Al** | **$Al_2$** ↓ **y** | $B_6$ |
| $Ni_{20}AlB_{14}$ | $Ni_{12}$ | $Ni_8$ | Al | **$(B_4)_2$** | $B_6$ |

At first sight, the existence of $B_4$ tetrahedra in the $\tau$-boride $Ni_{20}AlB_{14}$ seems to be very unusual; however, it is in accord with the geometrical situation, because $B_4$ tetrahedron and capped Friauf-polyhedron fit perfectly to each other. The B–B distances of 1.681(15) Å in the $B_4$ tetrahedron are comparable to those in $B_4Cl_4$ (1.65) Å[15] and $(t\mathrm{Bu})_4B_4$ (1.71 Å),[16] the only compounds in which $B_4$ tetrahedra have been proven by a structure analysis. Ni–B distances of 2.09 Å and 2.27 Å are similar to the values found for binary borides of nickel ($Ni_4B_3$,[17] NiB[18]). In addition, in this way the quite short distances between the Al atom in the center of the Friauf-polyhedron and the capping Ni atoms (2.411(1) Å) are avoided (Figure 2).

Solid-state compounds with tetrahedra of Group 14 elements and the heavier ones of Group 13 are well known and characterized (i.e. Zintl phases[19] with Al, Ga, In, Tl, Si, Ge, Sn, Pb). In contrast, $B_4$ tetrahedra have only been confirmed by structural analysis for the molecular compounds $B_4Cl_4$ and $(t\mathrm{Bu})_4B_4$. The formation of $B_4$ tetrahedra confirms the pronounced tendency of boron to form homonuclear bonds in solid-state compounds. Furthermore the example of $B_4$ tetrahedra in $Ni_{20}AlB_{14}$ shows that unusual structural units may be stabilized not only by special ligands as in molecular chemistry but also in a crystal structure if the structure–chemical conditions are fulfilled.

Finally investigations on the patterns of substitution of $\tau$-phases are of great importance for technical applications, because $\tau$-borides play an important role in the course of hardening processes of metallic materials by boriding[20] and in composites of ductile alloys and the extremely hard transition metal borides.[21]

## *Experimental Section*

$\tau$-phases of the system Ni/Al/B were synthesized by heating the elements to 1200–1300°C (Ar inert gas, corundum crucibles), slow cooling to 1000°C and quenching to room temperature. The phases were analyzed by X-ray diffraction on powdered samples. NiAl, $Ni_4B_3$, $Ni_2B$, and NiB were estabilished as border phases. The highest boron content obtained depends significantly on the temperature. Annealing at 900°C transforms a boron-rich sample ($a = 10.62$ Å) to a $\tau$-boride with lower boron content ($a = 10.56$ Å), NiB, and a still unknown phase (probably ternary). (This might explain the different findings of Kuz'ma et al. and Stadelmaier et al.). Single crystals suitable for structure analyses were only obtained when a small excess of aluminum was used; the latter evidently serves as a flux. Irregularly shaped and air-stable single crystals with metallic luster were isolated from the solidified melt.

Received: June 26, 1997
Revised version: November 19, 1997 [Z10602IE]
German version: *Angew. Chem.* **1998**, *110*, 981–983

**Keywords:** aluminum · borides · boron · nickel · structure elucidation

[1] a) "Borides: Solid State Chemistry": T. Lundström in *Encyclopedia of Inorganic Chemistry*, (Ed.: R. B. King), Wiley, Chichester, UK, **1994**; b) *Boron and Refractory Borides*, (Ed.: V. I. Matkovich), Springer, Berlin, **1977**.
[2] A. Westgren, *Nature* **1933**, *132*, 480–481.
[3] P. Villars, L. D. Calvert, *Pearson's Handbook of Crystallographic Data for Intermetallic Phases*, ASM, Metals Park, Ohio, **1985**.
[4] A. V. Gribanov, Yu. D. Seropegin, *J. Alloys Compd.* **1994**, *204*, L9–11.
[5] a) M. Andersson-Söderberg, Y. Andersson, *J. Solid State Chem.* **1990**, *85*, 315–317; b) V. Keimes, A. Mewis, *Z. anorg. allg. Chem.* **1992**, *618*, 35–38.
[6] Y. Khan, H. Wibbeke, *Z. Metallkde.* **1991**, *82*, 703–706.
[7] M. Ade, Dissertation, Universität Freiburg, **1997**.
[8] W. Jung, *Z. Kristallogr.* **1980**, *151*, 113–120.
[9] H. H. Stadelmaier, H. H. Davis, H. K. Manaktala, E.-T. Henig, *Z. Metallkde.* **1989**, *80*, 370–373.
[10] a) H. H. Stadelmaier, A. C. Fraker, *Metall* **1962**, *16*, 212–215; b) H. H. Stadelmaier, R. A. Draughan, G. Hofer, *Z. Metallkde.* **1963**, *54*, 640–644.
[11] N. F. Chaban, Y. B. Kuz′ma, *Inorg. Mater.* **1973**, *9*, 1886–1888.
[12] Structure analyses of $\tau$-phases in the system Ni/Al/B: irregular polyhedra with metallic luster $0.04 \times 0.04 \times 0.04$ mm; cubic, space group *Fm*3*m* (no. 225), $Mo_{K\alpha}$ radiation; Nonius-CAD4 diffractometer, graphite monochromator, $\omega/2\theta$-scan, $T = 293$ K, full-matrix least squares refinement, $Cr_{23}C_6$-type as a starting model [program SHELXL-93, G. Sheldrick, Universität Göttingen], all atoms were refined anisotropically except B atoms in $Ni_{20}AlB_{14}$; Lorentz- and polarization correction; empirical absorption correction using psi-scans. $Ni_{20.51(2)}Al_{2.49(2)}B_6$: $a = 10.4859(2)$ Å, $V = 1153.0$ Å$^3$, $2° < \theta < 35°$, 717 reflections measured, 160 independent reflections with $I > 0$, $\mu = 32.71$ mm$^{-1}$, $0.529 > t > 0.414$; 15 free parameters, $R1(F) = 0.014$ (157 reflections with $I > 2\sigma(I)$), $wR2(I) = 0.032$; $+0.64/-0.90$ e Å$^{-3}$, Ni1: $x = 0.38254(2)$, Ni2: 0.116938(2), B1: $x = 0.2733(3)$. $Ni_{20}Al_3B_6$: $a = 10.5110(4)$ Å, $V = 161.3$ Å$^3$; $2° < \theta < 40°$; 882 reflections measured; 217 independent reflections with $I > 0$; $\mu = 31.37$ mm$^{-1}$, $0.653 > t > 0.478$; 14 free parameters; $R1(F) = 0.073$ (193 reflections with $I > 2\sigma(I)$), $wR2(I) = 0.033$; $+1.90/-0.90$ e Å$^{-3}$, Ni1: $x = 0.38241(4)$, Ni2: $x = 0.16950(4)$, B1: $x = 0.2739(6)$. $Ni_{20}AlB_{14}$: $a = 10.6167(3)$ Å, $V = 1176.2$ Å$^3$; $2° < \theta < 40°$; 1040 reflections measured; 208 independent reflections with $I > 0$; $\mu = 30.73$ mm$^{-1}$, $0.746 > t > 0.546$; 16 free parameters; $R1(F) = 0.024$ (176 reflections with $I > 2\sigma(I)$) $wR2(I) = 0.065$; $+3.30$*$/-1.43$ e Å$^{-3}$ (* site 4b, probably an artefact as a result of crystal quality (broad reflection profiles), no atom could be refined on this site), Ni1: $x = 0.37978(4)$, Ni2: $x = 0.16903(3)$, B1: $x = 0.2758(7)$, B2: $x = 0.1940(5)$. Further details on the crystal structure investigations may be obtained from the Fachinformationszentrum Karlsruhe, D-76344 Eggenstein-Leopoldshafen, Germany (fax: (+49) 7247-808-666 (Frau S. Höhler-Schlimm); e-mail: crysdata@fiz-karlsruhe.de), on quoting the depository numbers CSD-408417, -408418, and -408419.
[13] W. P. Pearson *The Chemistry and Physics of Metals and Alloys*, Wiley Interscience, New York, **1972**.
[14] W. Biltz *Raumchemie der festen Stoffe*, Verlag Leopold Voss, Leipzig, **1934**.
[15] D. Thierry, Dissertation, Max-Planck-Institut für Festkörperforschung, Stuttgart, **1992**.
[16] T. Menneke, P. Paetzold, R. Boese, D. Blaser, *Angew. Chem* **1991**, *103*, 199–201; *Angew. Chem. Int. Ed. Engl.* **1991**, *30*, 172–174.
[17] S. Rundquist, S. Pramatus, *Acta Chem. Scand* **1967**, *21*, 191–194.

[18] S. Rundquist, *Acta Chem. Scand.* **1959**, *13*, 1193 – 1208.
[19] a) M. L. Fornasini, *Acta Crystallogr.* **1983**, *C39*, 943 – 946; b) C. Dohmeier, D. Loos, H. Schnöckel, *Angew. Chem.* **1996**, *108*, 141 – 161; *Angew. Chem. Int. Ed. Engl.* **1996**, *35*, 135 – 154; c) S. M. Kauzlarich, *Chemistry, Structure, and Bonding of Zintl Phases and Ions* VCH Publishers, New York, **1996**; d) H. Schäfer, B. Eisenmann, W. Müller, *Angew. Chem.* **1973**, *85*, 742 – 760; *Angew. Chem. Int. Ed. Engl.* **1973**, *12*, 725 – 743.
[20] a) R. Telle, *Chem. Unserer Zeit* **1988**, *22*, 93 – 99; b) E. Lugscheider, H. Reimann, R. Pankert, *Metall* **1982**, *36*, 247 – 251.
[21] C. B. Finch, P. F. Becher, M. K. Ferber, V. J. Tennery, C. S. Yust, *J. Cryst. Growth* **1982**, *58*, 647 – 655.

## Flavin- and Deazaflavin-Containing Model Compounds Mimic the Energy Transfer Step in Type-II DNA-Photolyases

Robert Epple and Thomas Carell*

DNA-photolyases are DNA-repair enzymes, which remove pyrimidine dimer lesions (which are cyclobutane derivatives) from the genome. These lesions are formed upon irradiation of cells with UV light.[1, 2] The basis of the repair reaction is a light-driven electron transfer from the enzyme to the dimer to form the radical anion, which subsequently monomerizes.[3] For the repair reaction DNA-photolyases need a reduced and deprotonated riboflavin cofactor as the electron donor, and they require a methenyltetrahydrofolate (MTHF) or an 8-hydroxy-5-deazaflavin as the second cofactor.[4] Model investigations show that deazaflavins are able to initiate the electron-transfer-driven repair as well, but with a very low quantum yield.[4, 5] Detailed enzymatic studies indicate, however, that the deazaflavin functions within the enzyme entirely as a photoantenna.[6] It transfers excitation energy to the reduced flavin. This energy transfer was shown to accelerate the repair rate and to shift the wavelength of maximal activity from 370 nm to 430 nm.[7]

Although such studies indicate that an efficient interaction of the reduced, deprotonated flavin and the oxidized deazaflavin, and therefore their close juxtaposition, would be desirable, time-resolved fluorescence data[8] and the X-ray crystal structures[9] of the *E. coli* photolyase and the *A. nidulans* photolyase revealed a surprisingly large cofactor separation of 16.8 Å and 17.5 Å (center-to-center distance), respectively. This unexpected finding raised speculation that the energy transfer is not rate-limiting and has never been optimized during evolution.[9, 10] In the photosynthetic apparatus, however, the large distance between the final antenna pigment and the electron donor is explained by the need to suppress a competing electron transfer from the electron donor to the antenna.[11] In order to study energy transfer processes between deazaflavins and flavins, to clarify the influence of the protonation state of the deazaflavin on the energy transfer, and to investigate electron transfer possibilities between both cofactors, we prepared a series of flavin- and deazaflavin-containing model compounds like **1** and **2** (Scheme 1).[12] The analysis of these model compounds provides insight into the interactions of both cofactors depending on their redox and protonation states.

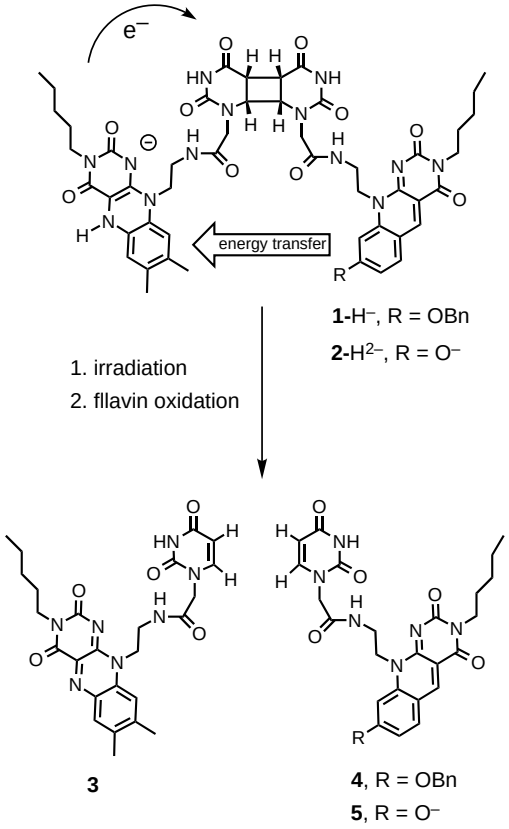


Scheme 1. The flavin- and deazaflavin-containing model compounds **1**-H$^-$ and **2**-H$^{2-}$ and its investigated photoinduced cleavage reaction to **3** – **5**.

The synthesis of the deazaflavin- and flavin/deazaflavin-containing model compounds **1**, **2**, and **6** – **8** is depicted in Scheme 2. For the preparation of the aminoethyl-substituted deazaflavin **9**, 6-chlorouracil **10** was treated with the Boc-protected ethylene diamine **11**.[13] Subsequent treatment of the product **12** with the bis-benzyl-protected 2,4-dihydroxybenzaldehyde **13**[14] afforded the deazaflavin **14**, which was alkylated to **15** with pentyl bromide to increase the solubility of the model compounds. Cleavage of the Boc group to yield **9** and reaction with the bis-carboxymethyl-substituted cyclobutane derivative, uracil dimer **16**,[12] afforded the bis-deazaflavin model compound **7**. Reaction of **16** with one equivalent of **9** and of the aminoethyl flavin **17**[12b,c] furnished the mixed flavin/deazaflavin-containing model compound **1**. In the model compounds **1** and **7** the 8-OH group of the deazaflavin moiety is benzylated, which prevents its deprotonation and therefore maintains the deazaflavin chromophore in the protonated "OH-form". Hydrogenolytic cleavage of the

[*] Dr. T. Carell, Dipl.-Natw. R. Epple
Laboratorium für Organische Chemie, ETH-Zentrum
Universitätstrasse 16, CH-8092 Zürich (Switzerland)
Fax: (+41) 1-632-1109
E-mail: tcarell@org.chem.ethz.ch

[**] This work was supported by the Swiss National Science Foundation and by the ETH Zurich. We thank J. Wytko-Weiss for a careful inspection of the manuscript and Prof. F. Diederich for his generous support.

  1433-7851/98/3707-0938 $ 17.50+.50/0 